ssdm'93

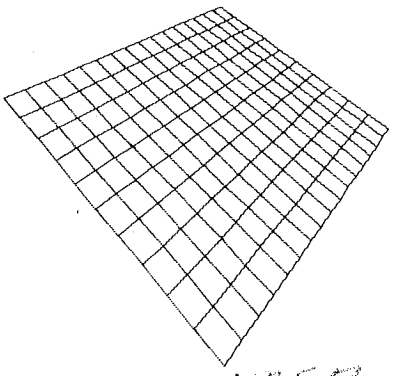

Very Long Wavelength Intersubband Infrared Hot Electron Transistor

S. D. Gunapala, J. K. Liu, T. L. Lin, and J. S. Park

Center for Space Microelectronics Technology
Jet Propulsion Laboratory, California Institute of Technology
4800 Oak Grove Drive, Pasadena, CA 91109, U.S.A.

Reprinted from Extended Abstracts of
the 1993 International Conference on Solid State Devices and Materials
August 29 - September 1, 1993, Nippon Convention Center, Makuhari Messe, Chiba, Japan

pp. 700-702

THE JAPAN SOCIETY OF APPLIED PHYSICS

Extended Abstracts of the 1993 International Conference on Solid State Devices and Materials, Makuhari, 1993, pp. 700-702

Very Long Wavelength Intersubband Infrared Hot Electron Transistor

S. D. Gunapala, J. K. Liu, T. L. Lin, and J. S. Park

Center for Space Microelectronics Technology
Jet Propulsion Laboratory, California Institute of Technology
4800 Oak Grove Drive, Pasadena, CA 91109, U.S.A.

We have demonstrated the first very long wavelength (16 μm) infrared hot electron transistor (IHET). This device utilizes the bound to continuum quantum well infrared photodetector (QWIP) as photosensitive emitter, a wide quantum well as base, and a thick $Al_xGa_{1-x}As$ barrier between the base and the collector as energy discriminating filter. This energy filter blocks the lower energy dark electrons, and is drain through the base while higher energy photo electrons pass to the collector. Therefore, the detectivity of the device at the collector is much higher than the detectivity at the emitter.

Very long wavelength infrared (IR) detectors and imaging systems are required in many space applications such as Atmospheric IR Sounder (AIRS) and Tropospheric Emission Spectrometer (TES) instruments which will be used in NASA's Earth Observation System (EOS). The wavelength of the infrared radiation required in these applications range from 3.7 to 15.4μm. These space applications have placed stringent requirements on the performance of the IR detectors and arrays including high detectivity, low dark current, uniformity and radiation hardness. This paper will present our study and development of a low dark current very long wavelength intersubband IR hot electron transistor (IHET).

There has been a lot of interest recently in the detection of very long wavelength (λ= 12-16 μm) infrared radiation using multiple quantum wells, due to the fact that these quantum well IR photodetectors[1] (QWIPs) and IHETs[2] can be fabricated using the mature III-V materials growth and processing technologies. This superior materials control results in high uniformity and thus allow fabrication of large staring arrays (λ= 8-12 μm) with excellent imaging performance[3]. One of the problems associated with the very long wavelength QWIPs is the higher dark current which adversely affects detector performance. By analyzing the dark current of shallow quantum wells we have realized that the total tunneling current (sequential tunneling + thermionic assisted tunneling) is significantly higher than the thermionic dark current (Fig. 1). The conduction electrons carrying these two tunneling current components are lower in energy than the photoelectrons[2]. Therefore, we have fabricated a 16μm $GaAs/Al_xGa_{1-x}As$ IHET which can effectively filter out sequential tunneling and thermionic assisted tunneling currents.

In this section we analyze the dark current of a single quantum well, which has intersubband absorption peak at 16 μm. First we have calculated the effective number of electrons[4] n(V) which are thermally excited into the continuum transport states, as a function of bias voltage V:

$$n(V) = \left(\frac{m^*}{\pi\hbar^2 L_p}\right)\int_{E_0}^{\infty} f(E)T(E,V)dE$$

The first factor containing the effective mass m* represents the average three dimensional density of states. Where L_p is the superlattice period, f(E) is the fermi factor $f(E) = [1+ \exp(E-E_0-E_F)/KT]^{-1}$, E_0 is the bound state energy, E_F is the two-dimensional fermi energy, E is the energy of the electron, and T(E,V) is the tunneling current transmission factor. This tunneling transmission factor obtained by applying WKB approximation to a biased quantum well is:

$$T(E) = (4\sqrt{E}\sqrt{(V_0 - E)} / V_0)e^{-2\tau}$$

where $\tau = (2L\sqrt{2m^*} / 3\hbar\Delta V)(V_0 - E)^{\frac{3}{2}}$, V_0 is the barrier height, ΔV is the bias voltage per superlattice period, and L is the barrier width. The number of electrons given by n(V) accounts for thermionic emission above the barrier height when $E>V_0$ and thermionic assisted tunneling and tunneling when $E<V_0$. Then we calculated the bias-dependent dark current $I_d(V)$, using $I_d(V) = eAn(V)v(V)$, where v(V) is the average transport velocity , A is the device area, and e is the electronic charge. The average transport velocity was calculated using $v(V) = \mu F[1+ (\mu F/v_s)^2]^{-1/2}$, where μ is the mobility, F is the electric field, and v_s is the saturated drift velocity. In order to obtained T = 60K bias-dependent dark current we have used μ = 1200 cm^2/V s, and $v_s = 5.5x10^6$ cm/s. Fig. 1 shows the T= 60K dark current due to thermionic emission, total dark current (thermionic + thermionic assisted tunneling + tunneling), and experimental dark

current of a QWIP sample which has wavelength cutoff λ_c = 17.8 μm. According to our calculations tunneling through the barriers dominate the dark current at temperatures below 30K, at temperatures between 40-60K thermionic assisted tunneling might becomes important, and at temperatures above 60K thermionic emission into the continuum transport states dominate the dark current.

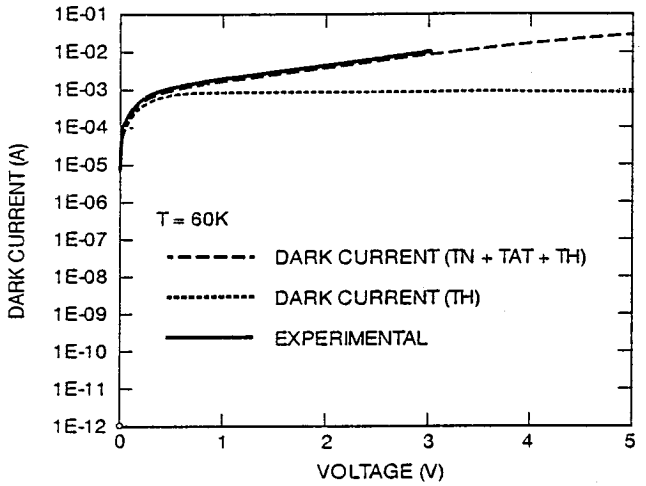

Fig.1 Theoretical and experimental (solid) dark current-voltage curves at T = 60K. Dotted curve shows the dark current (theoretical) due to thermionic emission only. Dashed curve shows the total dark current (thermionic + tunneling + thermionic assisted) versus bias voltage.

As shown in Fig. 2 the device structure consisted of a multi quantum well region of 50 periods of 500 Å undoped $Al_{0.11}Ga_{0.89}As$ barrier and 65 Å doped GaAs well. The quantum wells were doped to n = $5x10^{17}$ cm^{-3}, and sandwiched between a heavily doped (n = $1x10^{18}$ cm^{-3}) 1 μm GaAs contact layer at the bottom as the emitter contact and a doped (n = $3x10^{17}$ cm^{-3}) 500 Å GaAs layer on the top as the base contact. On top of the base a 2000 Å undoped $Al_{0.11}Ga_{0.89}As$ layer and a doped (n = $3x10^{17}$ cm^{-3}) 0.5 μm GaAs layer were grown. The 2000 Å undoped $Al_{0.11}Ga_{0.89}As$ As layer acts as a discriminator between the tunnel-electrons and photo-electrons, and the top 0.5 μm GaAs layer serves as the collector. This device structure was grown on a semi-insulating GaAs substrate using molecular beam epitaxy.

The intersubband absorption was measured on a 45° polished multipass waveguide as shown in the inset of Fig. 3. As shown in the Fig. 3 the T = 300K absorption coefficient spectra α_p has a peak infrared absorption coefficient α_p= 534 cm^{-1} at λ_p= 17.1 μm with absorption half heights at 14.2 and 18 μm (i.e., a full width at half maximum of $\Delta\lambda$ = 3.8 μm). At low temperature the half width narrows and the peak absorption coefficient increases by a factor of 1.3 so that α_p = 694 cm^{-1} at T = 60K corresponding to an unpolarized quantum efficiency $\eta = (1-e^{-2\alpha\ell})/2 =$ 16.5%.

To facilitate the application of bias to the quantum well structure, the following processing steps were carried out. First we have chemically etched

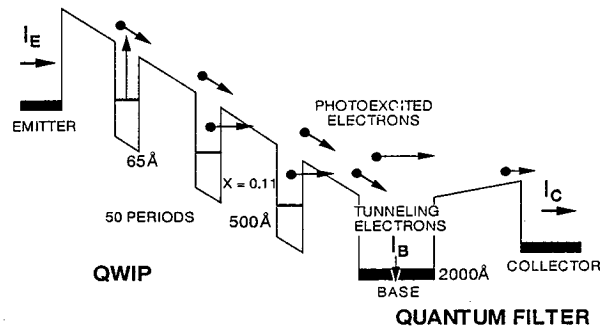

Fig.2 Conduction-band diagram of a infrared hot electron transistor, which utilizes bound to continuum intersubband transition.

arrays of 200x200 μm^2 square collectors. In the next processing step we have etched the $6.25x10^{-4}$ cm^2 QWIP mesas which overlap with collector mesas. Finally, Au/Ge ohmic contacts were evaporated onto the emitter, base and collector contact layers. The emitter and collector dark currents versus base-collector bias voltage are shown in Fig. 4. This figure also shows the lower energy dark current filtration capability of the quantum filter. The dark current transfer ratio $\left(\alpha_d = I_{C(dark)} / I_{E(dark)}\right)$ is $7.2x10^{-5}$ at operating base-collector bias voltage V_{CB} = -42 mV.

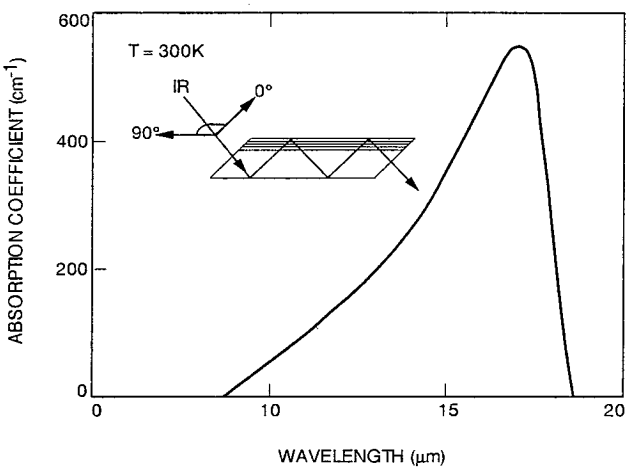

Fig.3 Absorption coefficient spectra $\alpha(\lambda)$ of the long wavelength quantum well infrared detector. This absorption spectra was measured at room temperature using a 45° multipass waveguide geometry as shown in the inset.

These 200x200 μm^2 square detectors were back illuminated through a 45° polished facet as described in detail previously[1] and responsivity spectra were measured with a tunable source consisting of a 1000K blackbody and a grating monochromator. The Responsivity spectrum measured at T = 60K is shown in Fig. 5. The values of the peak wavelength λ_p, cutoff wavelength λ_c and the spectral width ($\Delta\lambda / \lambda$) (full width at half maximum) are 16.3 μm, 17.3 μm and 20% respectively. The absolute responsivity was measured by two different methods, comparison with calibrated pyroelectric detector and, using a calibrated blackbody source. The peak responsivity Rp of the detector was 400 mA/W, while the peak responsivity and the shape

of the spectra were independent of the measuring technique as expected. Fig. 6 shows the IHET emitter and collector photo currents versus base-collector voltage at T = 60K. Emitter was kept at -1V bias relative to the base potential. Due to the hot electron relaxation in the wide base region, the photo current at collector is smaller relative to the emitter photo current.

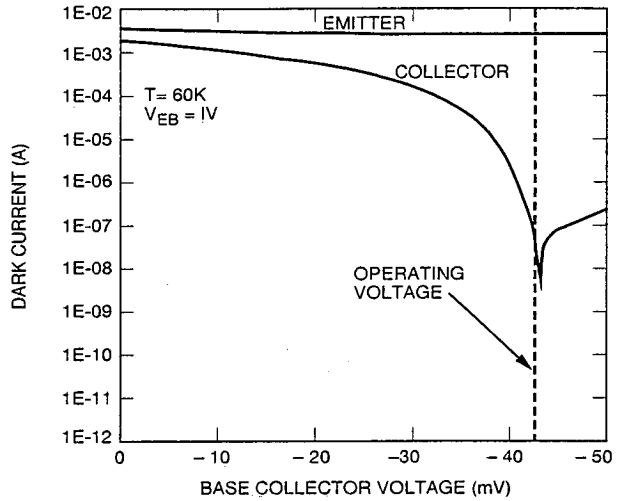

Fig.4 IHET emitter and collector dark currents versus base-collector voltage at T = 60K. Emitter bias was kept at -1V relative to the base potential. This figure also shows the lower energy dark current filtration capability of the quantum filter.

Photo current transfer ratio $\left(\alpha_p = I_{C(photo)} / I_{E(photo)}\right)$ is $1.2x10^{-1}$ at V_{CB} = -42 mV. It is worth to notice that α_d is more than three orders of magnitude smaller than α_p.

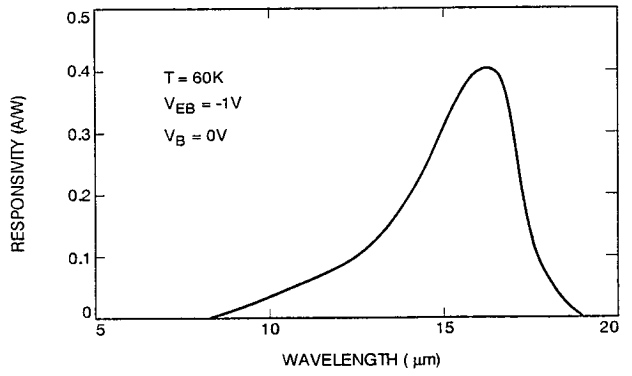

Fig.5 Responsivity spectra between emitter and base at T = 60K. Emitter was kept at -1V bias relative to the base.

The optical gain g of the detector determined from $R = (e/h\nu)\eta g$ is given by g = 0.2. The noise current i_n was calculated using $i_n = \sqrt{4eI_d g\Delta f}$, where Δf is the bandwidth. The calculated noise current of the detector is i_n = 17 pA at T = 60K. The peak D^* can now be calculated from $D^* = R\sqrt{A\Delta f}/i_n$. The calculated D^* between the emitter and the base (QWIP) at V_{EB} = -1V, V_{CB} = -42 mV and T = 60K is $5.8x10^8$ cm$\sqrt{Hz}$/W. The detectivity D^* at the collector (IHET) is

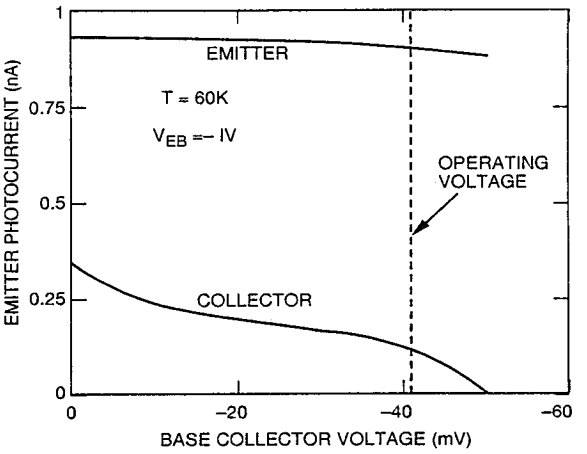

Fig.6 IHET emitter and collector photo currents Vs base-collector voltage at T = 60K. Emitter was kept at -1V bias relative to the base potential.

determined[5] from $D^*(IHET) = (\alpha_p/\sqrt{\alpha_d})\, D^*(QWIP)$ is given by $D^*(IHET) = 8.2x10^9$ cm$\sqrt{Hz}$/W at T = 60K.

In conclusion, we have demonstrated the first very long wavelength (λ_c = 17.3 μm) IHET. This device clearly shows the dark current filtration capability of the energy filter. Therefore, the D^* of IHET is much higher than the D^* of two terminal multi quantum well detector.

The research described in this paper was performed by the Center for space Microelectronics Technology, and was jointly sponsored by Ballistic Missile Defense Organization/Innovative Science and Technology Office, and the National Aeronautics and Space Administration, Office of Advanced Concepts and Technology.

REFERENCES

1) B. F. Levine, C. G. Bethea, G. Hasnain, J. Walker, and R. J. Malik, Appl. Phys. Lett. 53 (1988) 296 (and references therein).

2) K. K. Choi, M. Dutta, P. G. Newman, and M.-L. Saunders, Appl. Phys. Lett. 57 (1990) 1348 (and references therein).

3) B. F. Levine, C. G. Bethea, K. G. Glogovsky, J. W. Stayt, and R. E. Labenguth, Semicon. Sci. Technol. 6 (1991) c114.

4) B. F. Levine, C. G. Bethea, G. Hasnain, V. O. Shen, E. Pelve, R. R. Abbot, and S. J. Hsieh, Appl. Phys. Lett. 56 (1990) 851.

5) K. K. Choi, M. Taysing-Lara, L. Fotiadis, and W. Chang, Appl. Phys. Lett. 59 (1991) 1614.